








# A Three-Fingered Force Feedback Glove Using Fiber-Reinforced Soft Bending Actuators

Ziqi Wang , Dangxiao Wang , Senior Member, IEEE, Yu Zhang , Jiaqi Liu , Li Wen ,  
Weiliang Xu , Senior Member, IEEE, and Yuru Zhang , Senior Member, IEEE

**Abstract**—Force feedback gloves are promising for producing immersive haptic sensations in virtual reality systems or for intuitive control of remote robots in dexterous manipulation tasks. Existing gloves mainly adopt rigid actuators. In this article, we propose a force feedback glove using pneumatically powered fiber-reinforced soft bending actuators. Based on the unilateral deformable feature of the soft actuator, a dorsal-side mounted soft-rigid linkage mechanism is proposed to produce fingertip force feedback. We incorporated and experimentally determined a positive prebending deformation of the actuator to ensure small backdrive forces for simulating free-space sensation. To enable a large workspace of the glove, the soft-rigid linkage is synthesized to ensure full open/closure of the finger without any mechanical interference. Using a modular design concept, a three-fingered glove prototype is developed with a mass of 93.7 g. Experimental results show that the glove can provide distinct force feedback between free and constrained space. For free space, the maximum backdrive force is 0.48 N, while the fingertip force reaches up to 4.09 N for simulating the constrained space. Experiments also indicate that the glove is easy to put on/off. These results illustrate the feasibility of developing light-weighted force feedback gloves using fiber-reinforced soft bending actuators.

**Index Terms**—Force feedback, grasping, haptic interface, pneumatic actuators, soft robotics.

Manuscript received December 19, 2018; revised April 5, 2019; accepted June 5, 2019. Date of publication July 1, 2019; date of current version April 30, 2020. This work was supported by the National Key Research and Development Program under Grant 2017YFB1002803. (Corresponding author: Dangxiao Wang; Li Wen.)

Z. Wang, Yu. Zhang, and Y. Zhang are with the State Key Lab of Virtual Reality Technology and Systems, Beijing Advanced Innovation Center for Biomedical Engineering, Beihang University, Beijing 100191, China (e-mail: wzqzq1997@qq.com; 13020031535@163.com; yuru@buaa.edu.cn).

D. Wang is with the State Key Laboratory of Virtual Reality Technology and Systems, Beijing Advanced Innovation Center for Biomedical Engineering, Beihang University, Beijing 100191, China, and also with the Peng Cheng Laboratory, Shenzhen 518055, China (e-mail: hapticwang@buaa.edu.cn).

J. Liu and L. Wen are with the Biomechanics and Soft Robotics Lab, Beihang University, Beijing 100191, China (e-mail: jiaqiliu@buaa.edu.cn; liwen@buaa.edu.cn).

W. Xu is with the Department of Mechanical Engineering, University of Auckland, Auckland 1010, New Zealand (e-mail: p.xu@auckland.ac.nz).

This article has supplementary downloadable material available at <http://ieeexplore.ieee.org>, provided by the authors.

Color versions of one or more of the figures in this article are available online at <http://ieeexplore.ieee.org>.

Digital Object Identifier 10.1109/TIE.2019.2924860

## I. INTRODUCTION

IN RECENT years, the invention of low-cost head-mounted displays such as Oculus Rift has advanced the development of virtual reality interaction, which proposes a strong motivation for wearable haptic feedback devices. In order to increase the immersive feeling of interaction with the virtual world, a haptic feedback device should allow users to touch and manipulate virtual objects intuitively and directly, through utilizing the dexterous manipulation and sensitive perception capabilities of our hands. Force feedback gloves are a promising solution to produce an immersive haptic sensation in virtual reality systems.

In the past two decades, many force feedback gloves have been developed [1]–[12]. CyberGrasp is a representative commercial one [4]. With a 450 g exoskeleton mounted on the back of the hand, the glove can provide up to 12 N forces to the fingertips. Rutgers Master II—New Design used linear pneumatic pistons distributed in the palm to provide forces between the palm and fingers [9]. Pistons are directly attached to the fingers and provides up to 16 N forces to each fingertip. HIRO III can provide a large force output and even simulate the gravity of virtual objects [1]. Choi *et al.* [13] developed a lightweight device that renders a force directly between the thumb and three fingers, and thus, to simulate objects held in pad opposition type grasps. Details about available force feedback gloves are described in one recent survey on wearable haptic devices [14], which presented a taxonomy and review of wearable haptic systems for the fingertip and the hand, focusing on those systems directly addressing wearability challenges. Another survey summarized the pros and cons of existing design solutions to the major subsystems of a haptic glove including sensing, actuation, control, transmission, and structure [15]. Overall, most existing gloves adopt rigid actuators and, thus, have limitations such as safety and uncomfortable sensations when the rigid components directly contact users' skin.

Recently, soft actuators have been introduced into haptic devices, aiming to improve the wearability, safety, and comfortable sensation of the device [16]–[19]. Compared to rigid actuators, soft actuators fit well in the applications that involve direct contact with human skin. Jadhav *et al.* [20] developed a glove based on a soft exoskeleton with reduced thickness at users' finger joints, and McKibben muscles are used to pull a string on the top of the exoskeleton to mimic a bell-crank lever mechanism. Yun *et al.* [21] developed an assembly-based soft pneumatic assistive glove (Exo-Glove PM), in which a hybrid actuator

module consisting of a soft actuation structure and rigid joining methods were utilized to provide force feedback on fingertip. Using the jamming principle, Zubrycki *et al.* [10] developed a haptic glove for simulating the sensation of grabbing and holding an object. They presented the concepts of jamming tubes or pads for simulating grasping tasks, illustrating a solution of a soft, mechanically simple, and intrinsically stable mechanism for haptic gloves.

Among various soft actuators, soft fiber-reinforced bending actuators have a unique feature of a simple tubular geometry that offers ease of manufacture [18]. By arranging fibers along their length, these actuators can produce nontrivial deformation modes. Besides, a strain-limiting layer added to one side enables unilateral bending when inflating the air into it. These actuators have been used for designing hand rehabilitation gloves [18], [22], [23]. While soft fiber-reinforced bending actuators can provide controllable deformation in response to the inflated air pressure, one open question for building a force feedback glove using these actuators is how to meet the contradictive requirements from simulating both free and constrained spaces. In one aspect, for simulating free space haptic interactions, the back drivability of the glove should be ensured when these actuators are mounted on fingers. In the other aspect, sufficient feedback forces should be provided on fingertips for simulating constrained space haptic interactions, and also ensure no interference between the glove's mechanical structure and users' fingers.

In our previous work [24], we proposed a solution to design a force feedback glove using soft fiber-reinforced bending actuators. The glove has a soft-rigid coupled linkage placed as dorsal side of the hand. In this article, to ensure small backdrive forces for simulating free-space sensation, a positive prebending deformation of the actuator is incorporated and experimentally determined; and to ensure a large workspace of the glove, the soft-rigid linkage is synthesized to ensure full open/closure of the finger without any mechanical interference. Using a modular design concept, a three-fingered glove prototype is developed with a mass of less than 100 g and experimental results show that the glove can provide distinct force feedback between free and constrained space.

## II. DESIGN OF THE SOFT-RIGID COUPLED GLOVE

### A. Design Goals

Similar to the three criteria proposed by Salisbury for a desktop force feedback device [25], a force feedback glove should also meet the contradictive requirements of free space and constrained space simulations, i.e., free space must feel free, and solid objects must feel stiff.

To simulate the free-space sensation, the resistance of the glove should be as small as possible. The glove needs to be light weighted. All the kinematic pairs should have low friction. In order to simulate diverse grasping gestures, the glove should allow free open/close of fingers without interference between the mechanism and fingers.

To simulate the constrained space sensation, the magnitude of simulated force should be large enough to simulate daily grasping tasks, and the simulation error of the applied force on

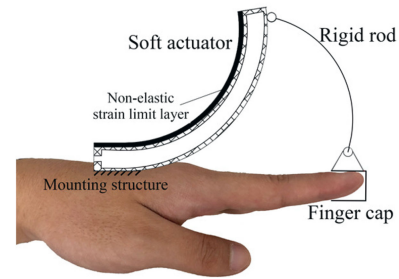


Fig. 1. Concept of the glove using a soft-rigid coupled mechanism.

fingertips should be less than the discrimination threshold of human perception on force magnitude.

Furthermore, the glove should be easy to adapt to different hand size, and easy to put ON and OFF.

### B. Dorsal-Side Soft-Rigid Coupled Solution

To meet the contradictive demands of simulating both the free space and the constrained space, as shown in Fig. 1, we propose a soft-rigid coupled solution of combining a soft bending actuator and a linkage mechanism with only one rigid link. The key concepts of the proposed solution include the following three aspects.

First, by exploiting the unilateral deformable feature of the soft actuator provided by the strain-limiting layer and the radial fiber reinforcements, a dorsal-side mounting solution with a prebending of the soft actuator is proposed to enable the back-drivability performance and simulate the free-space sensation. As the soft actuator is installed on the dorsal side, this solution allows full open and closure gestures of the users' hand. The strain limiting layer (i.e., the black and bold line on the top of the actuator in Fig. 1) is mounted on the top surface of the actuator, which ensures the distance between the user's fingertip and the actuator's tip becomes larger when the air is inflated into the actuator. In simulating constrained space, the actuator is inflated with pressured air. The actuator is bent to pull the rigid rod, and an active force is then transmitted along the linkage mechanism to users' fingertip.

Second, a single-link mechanism with a curve-shaped rigid rod is proposed to transmit the force from the actuator to users' fingertip. In order to reduce the joint friction and weight caused by the mechanism, we aimed to use as fewer links and kinematic pairs as possible to transmit the force. Therefore, a single link solution is used to connect the fingertip and the end of the soft actuator, and only two kinematic pairs (i.e., the revolution joints) are utilized in the proposed soft-rigid coupled mechanism. The shape and size of the connecting rod is carefully designed to make sure it will not interfere with the motion of adjacent fingers. The proposed mounting solution can ensure no interference between the adjacent fingers during grasping.

Third, a prebending of the soft actuator is used to ensure the free space simulation performance. In simulating free space, the user is able to move the finger freely and the resistance of the gloves should be as less as possible. We applied a prebending of the soft actuator to enable the back-drivability performance

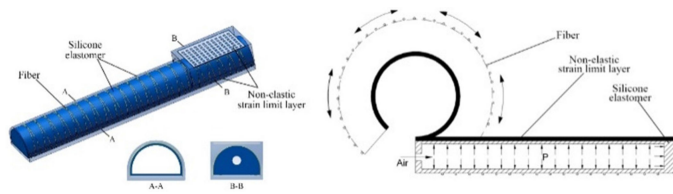


**Fig. 2.** Inflation of a soft actuator with strain limiting layer and radial reinforcement. (a) Three-dimensional illustration. (b) Bending with inflated air.

for simulating the free-space sensation. When the actuator is not inflated by air pressure, the soft-rigid mechanism can freely bend in response to the rotation of the finger.

### C. Design of the Soft Bending Actuator

In this section, after briefly introducing the working principle of the soft bending actuator, the material and geometric parameters of the soft bending actuator are determined. Then, the prebending value of the soft actuator is determined to enable the back-drivability performance for simulating the free-space sensation.

**1) Material and Geometric Design of the Actuator:** As shown in Fig. 2, the soft bending actuators are composite tubular constructions consisting of anisotropic fiber reinforcements and strain limiting layer in an elastomeric matrix [18].

The force output performance of the soft actuator depends on the following factors: the material of the software actuator; the shape and parameters of the air cavity; and the material of the strain limiting layer; and the material of the tensioning fiber.

The main body of the soft actuator is the silicone elastomer (Mold Star 30), which expands uniformly when the inside elastic cavity is inflated with pressured air. The material can bear a pressure of 180 kpa, and the maximal output force is 4-5 N.

Radial reinforcements were added to the main body to limit its inflation in a radial direction. By wrapping the main body with Kevlar silk, the expansion in the radial direction of the main body can be limited and the expansion in the axial direction can be increased. At the same time, the intension of the actuator can intensify.

Furthermore, a strain limiting layer (i.e., fiberglass) was applied to the flat surface of the main body. Although the material of the main body is isotropic, by gluing the nonelastic strain limit layer, the main body becomes anisotropic, so it can expand in just one direction. After gluing the fiber-glass-mesh to limit the direction of one side of the actuator, the other side of the actuator expands more. Therefore, the actuator bends when the inside elastic cavity is inflated with air pressure, as shown in Fig. 2(b).

The cross-sectional shape is an important parameter to determine the output force of the actuator. Previous work on soft actuators found that semicircular shape produces larger bending angles with the same air pressure than rectangular and circular shapes [26]. Therefore, we adopted the semicircular shape for the internal cavity of the soft actuator. Furthermore, a rectangular cross-sectional area was designed at the fixed end of the

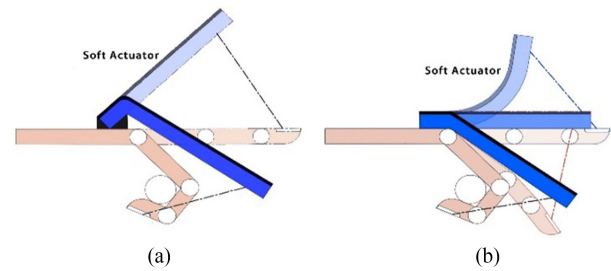


**Fig. 3.** Comparison before and after introducing a positive prebending deformation. (a) Actuator has no bending deformation at the full extension state and negative bending at the full grasping state. (b) Actuator has positive bending at the full extension state, no bending at the intermediate state, and negative bending at the full grasping state.

actuator, which is convenient for fixation of the actuator on the dorsal surface of the users' palm.

Furthermore, a larger radius of the semicircular shape and a bigger length of the actuator leads to a larger bending deformation. The greater the wall thickness, the smaller the bending deformation is. In the other aspect, the width of the actuator needs to be smaller than the width of the user's finger, and thus, to avoid interference among adjacent fingers. The length of the actuator should be compatible with the length of the finger. Considering these effects, the geometric parameters of the actuator were determined.

**2) Prebending of the Soft Actuator:** When the glove is used for simulating free space, the resistance exerted on the fingertip should be sufficiently small throughout the workspace of finger movement. The force is directly related to the bending deformation of the soft actuator.

To explain the change of the actuator's shape, we define two different types of bending deformation: positive bending and negative bending. The former means that the actuator bends to the side of the strain limiting layer, while the latter toward the opposite side.

As illustrated in Fig. 3(a), we define two states during the flexion/extension process of a finger: full extension and full grasping (i.e., grasping a cylindrical object with a diameter of 20 mm). When the bending deformation of the actuator is zero at the full extension state, the actuator keeps producing a negative bending during the grasping process. With the increase of the negative bending deformation, the actuator produces a bigger and bigger pushing force on the fingertip, which may greatly reduce the free-space sensation.

In order to obtain a smaller resistance throughout the workspace of finger movement, we incorporate a positive prebending at the full extension state. It should be noted that there is no inflated air pressure in the actuator when using the force feedback gloves in simulating free space. The mechanical assembly formulates the prebending.

By introducing the positive prebending deformation, we can obtain three states, as shown in Fig. 3(b). In addition to the two states of full extension and full grasping, an intermediate state is defined to reflect the critical change of the bending deformation of the soft actuator. In this state, the bending is zero. In contrary, in the full extension and grasping state,



the actuator has the largest positive and negative bending, respectively.

When the finger rotates from the full extension state to the intermediate state, the soft actuator produces a push force on the finger nail. This force is harmful for the free-space sensation. With the increase in the finger's rotating angle, the amount of the positive bending decreases, and the magnitude of the harmful force decreases. After the finger arrives at the intermediate state, the bending becomes zero. Then, when the finger rotates from the intermediate state to the full grasping state, the actuator produces a push force on the fingertip. This force is also harmful for the free-space sensation. With the increase in the finger's rotating angle, the amount of the negative bending increases, and the magnitude of the harmful force increases.

In order to ensure the free-space sensation, the magnitude of the abovementioned harmful force should be smaller than a predefined threshold. Although it is hard to provide a strict threshold for the resistance force of a haptic device to ensure a satisfied free-space sensation, referring to Phantom desktop device, we proposed the design specification of 1 N back drive force for our glove. Because the bending of the actuator directly determines the magnitude of the force, we performed a pilot experiment to determine the bending values of the actuator at the two extreme states based on the allowable resistance force in simulating free-space sensation. The details of the experiment are explained in Section V-A.

#### D. Parameter Synthesis of the Mechanism

When designing the rigid rod for transmitting the actuating force from the tip of the soft actuator to the fingertip, two parameters were considered: the length and the shape.

Because the rod is rigid, no matter what shape of the rigid rod is, the distance between the end of the actuator and the fingertip is constant. The allowable length of the rigid rod was determined by the distance between the end of the actuator and the fingertip, while  $l_{AB}$  and  $l_{A'B'}$  is the length of the rod in the full extension and grasping state, respectively,

$$\begin{cases} l_{AB} = \sqrt{(x_A - x_B)^2 - (y_A - y_B)^2} \\ l_{A'B'} = \sqrt{(x_{A'} - x_{B'})^2 - (y_{A'} - y_{B'})^2} \end{cases} \quad (1)$$

In order to simulate the grasping of a smaller cylinder, the length  $l_{A'B'}$  needs to be larger. When the diameter of the virtual object is greater than a predefined value  $d^*$ , the following relationship is always satisfied:

$$l_{AB} \geq l_{A'B'}. \quad (2)$$

In this case, the length of the rigid rod can be chosen as any value in the following range:

$$l_{A'B'} \leq L \leq l_{AB}. \quad (3)$$

Two steps determine the length of the rod. First is to make sure no interferences between the rod and the user's finger during the whole movement range of the finger. The other is to produce as small resistance force as possible in the free space simulation. The length of the rigid rod will directly influence

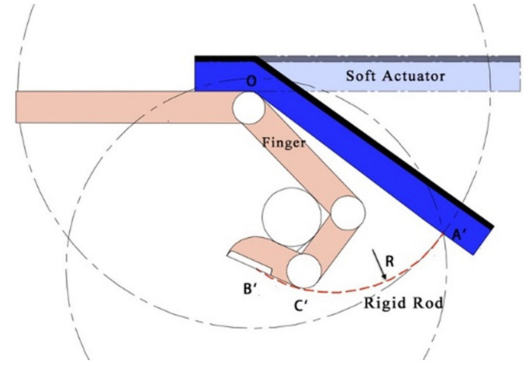


Fig. 4. Derive the radius of the arc-shaped rod based on the position of the three key points ( $A'$ ,  $B'$ ,  $C'$ ).

the resistance of the feedback glove in free space. Due to the unilateral deformation structure of the soft bending actuator, the nondeformed limiting layer is not easy to be bent. The longer the rigid rod is, the smaller the resistance is in free space. Therefore, the maximum length (i.e.,  $l_{AB}$ ) is selected from the range defined in (3).

After determining the length of the rod, we need to determine its shape. Generally speaking, two criteria are considered, one is easy to be manufactured, and the other being to ensure no interference between the rod and the finger throughout the movement workspace of the finger.

For the first criterion, simple shape is logical. In order to ensure easy fabrication and avoid stress concentration, the arc shape was chosen. For the second criterion of avoiding interference, the worst case occurs when the finger is at the full grasping state (i.e., grasping a cylindrical object with a diameter of 20 mm). When there does not exist an interference at this state, no interference occurs at any other configurations of the finger.

As shown in Fig. 4, a schematic is utilized to derive the radius of the arc-shaped rod based on the position of the three key points ( $A'$ ,  $B'$ ,  $C'$ ). When the finger is in grasping state and the equivalent length of the rigid rod  $L = l_{AB}$ , the position of the actuator end is point  $A'(x_{A'}, y_{A'})$ . The position of  $A'$  can be determined by drawing, i.e.,  $A'$  is the intersection of the two circles. The point  $B'(x_{B'}, y_{B'})$  is the center point of the revolute joint between the rod and the finger cap. At the critical state where the rigid link interferes with the finger, the point  $C'(x_{C'}, y_{C'})$  is right on the arc where the link lies.

After determining the three points ( $A'$ ,  $B'$ ,  $C'$ ) on the arc, the radius  $R$  of the arc can be determined as

$$R = \frac{\sqrt{D^2 + E^2 - 4F}}{2} \quad (4)$$

where

$$\begin{cases} D = \frac{(x_B^2 + y_B^2 - x_{A'}^2 - y_{A'}^2)(y_{B'} - y_{C'}) + (x_B^2 + y_B^2 - x_{C'}^2 - y_{C'}^2)(y_{A'} - y_{B'})}{(x_{A'} - x_{B'})(y_{B'} - y_{C'}) - (x_{B'} - x_{C'})(y_{A'} - y_{B'})} \\ E = \frac{(x_B^2 + y_B^2 - x_{A'}^2 - y_{A'}^2)(x_{B'} - x_{C'}) + (x_B^2 + y_B^2 - x_{C'}^2 - y_{C'}^2)(x_{A'} - x_{B'})}{(x_{B'} - x_{C'})(y_{A'} - y_{B'}) - (x_{A'} - x_{B'})(y_{B'} - y_{C'})} \\ F = -x_{A'}^2 - y_{A'}^2 - Dx_{A'} - Ey_{A'} \end{cases} \quad (5)$$

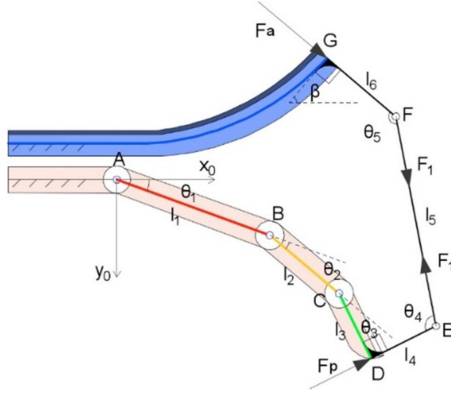


Fig. 5. Schematic diagram for constructing the kinematic model.

### III. ANALYSIS OF THE SOFT-RIGID COUPLED GLOVE

#### A. Force Analysis

In order to control the glove, it is necessary to derive the relationship between the fingertip force and the air pressure, considering the effect of the finger configuration on the relationship. To do so, we made several assumptions as follows.

- 1) All the links move in the same plane.
- 2) All the forces are found at the equilibrium.
- 3) The forces in hinges, at the fingertip, and at the tip of the actuator all act at a single point.
- 4) The weights of all the links are ignored.

For the sake of the analysis, a reference coordinate system is set up, as shown in Fig. 5. The origin is at point A and  $x$ -axis is parallel to the finger's phalanges when the finger is at the full extension state.

As shown in Fig. 5, the normal force perpendicular to the users' fingertip can be derived as

$$F_p = -F_1 \cos \theta_4 \quad (6)$$

where  $F_1$  is the force internal to the link EF, and the direction of the internal force is always as same as the direction of the rod, and the internal force on the point E is always equal to the internal force on the point F. The magnitude of the  $F_1$  can be computed as follows:

$$F_1 = F_a \cos (180 - \theta_5) \quad (7)$$

where  $F_a$  is the resistance produced by the active bending of the actuator, which can be expressed as

$$F_a = g(p, x_G, y_G, \beta) \quad (8)$$

where  $p$  is the air pressure inflated into the actuator,  $(x_G, y_G)$  is the position of the actuator's tip, and  $\beta$  is the bending angle of the actuator with respect to the  $x$ -axis.

As the mechanical behavior of the soft actuator is nonlinear, it is not a trivial task to derive an analytic model. Therefore, finite element analysis (FEA) is used to derive the model in (8). As shown in (6), the normal force ( $F_p$ ) on the fingertip is determined by the product of internal force  $F_1$  and the angle  $\theta_4$ . The detailed control procedure is as follows.

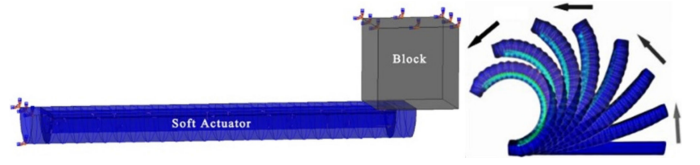


Fig. 6. FEA simulation of the fiber-reinforced soft actuator.

TABLE I  
SIMULATION RESULTS

p (kPa)	9.99	23.475	49.546	72.92	88.428
Fa (N)	0.058	0.141	0.368	0.503	0.645
p (kPa)	115.62	136.97	149.78	159	178.55
Fa (N)	0.916	1.09	1.218	1.314	1.522

- 1) Given the fingertip force command computed by the force rendering algorithm, we can compute the internal force  $F_1$  based on the measured angle  $\theta_4$ .
- 2) Compute the required actuation force  $F_a$  based on (7).
- 3) Compute the air pressure based on the inverse model of (8).
- 4) Low-level control to produce the required air pressure: The air pressure is modulated by controlling the voltage of the electro-pneumatic regulator.

When the user's hand is performing a grasping operation, the angle  $\theta_4$  is not a constant value. In order to accurately control the  $F_p$ , we need to measure the angle in real time. The accuracy of the fingertip force mainly dependent on the measurement accuracy of the angle and on the inverse mechanics model of the soft actuator, which is constructed by the FEM simulation. The details are provided in the following section.

#### B. FEA Analysis of the Soft Actuator

For the FEA simulation, the tube of the soft actuator, which is semicircular shaped, was fabricated with silicone elastomer (Mold Star 30). Two ends of the half cylinder are sealed by two caps, separately. Then, Kevlar wires are used to restrain the radial expansion, and a Nylon layer is fixed on the bottom of the tube to restrict the extension. In the FEA simulation, the material coefficients of the silicone elastomer are  $C1 = 0.14957$ ,  $C2 = 0.037393$ . The Young's modulus and the Poisson ratio of the Kevlar wires are 31067 MPa and 0.36, respectively. The radius of the semicircular shape is 9 mm, while the length is 110 mm, and the wall thickness of 3 mm.

The three-dimensional (3-D) model of the soft actuator was then imported into ABAQUS/Standard with one side of the actuator fixed. The pressures ranging from 0 to 180 kPa were applied to the inner chamber. The deformations of the end of the soft actuator under different air pressure are shown in Fig. 6.

It should be noted that the nonelastic strain of the actuator was ignored in the simulation, which might lead to the deviation between the simulation and the experimental results. The simulated  $p$ - $F_a$  relation was shown in Table I. The error of the FEA simulation will be evaluated in Section V-A.

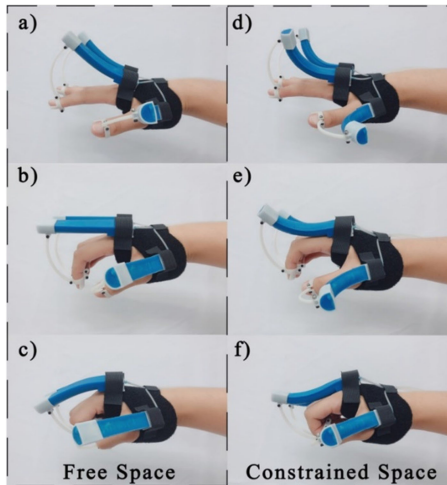


**Fig. 7.** Snapshots of the glove. (a) Full extension state in free space. (b) Intermediate state in free space. (c) Full grasping state in free space. (d) Full extension state in constrained space. (e) Intermediate state in constrained space. (f) Full grasping state in constrained space.

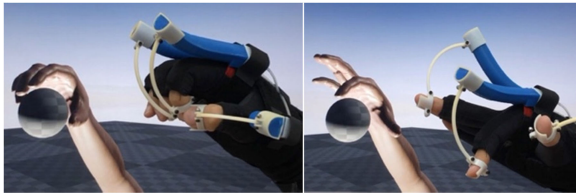


**Fig. 8.** Grasping a ball in virtual environment with different gestures.

#### IV. PROTOTYPE GLOVE

A prototype three-fingered glove is developed using a modular concept, where the three soft actuators were mounted on the thumb, the index, and the middle finger. They were placed on the dorsal of the hand using a Velcro with its length being adjustable to the different-sized hands. The rigid rod is made by 3-D printing, and the materials used are resin, which ensures sufficient stiffness and is lightweight. The weight of all parts on each finger is 31.23 g.

**Fig. 7(a)–(c)** show the snapshot of the fingers moving in the free space. The workspace of the glove is sufficiently large, and the fingers can rotate in a large range to simulate full grasping scenarios. In **Fig. 7(c)**, the actuator only produces a small bending angle compared to its original configuration (i.e., zero bending state). This result validates the effectiveness of the prebending approach, which ensured the free bending of the soft actuator to enable the back-drivability performance and simulate the free-space sensation. In the supplementary video, it clearly shows that the user can move all fingers freely when the soft actuator was not pressurized. **Fig. 7(d)–(f)** shows the snapshot of the fingers moving in the constrained space, where the unilateral bending deformation of the actuator produces resistance forces on users' fingertip.

As shown in **Fig. 8**, the glove was integrated with a head-mounted display to enable users to experience the haptic sensation of grasping virtual objects. In the supplementary video, it clearly shows that the soft actuator became rigid whenever

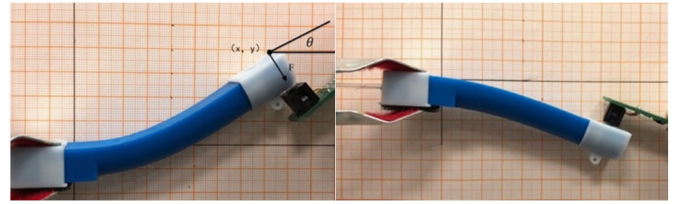


**Fig. 9.** Experiment to measure the resistance force of the actuator under no air pressure. (a) Positive bending. (b) Negative bending.

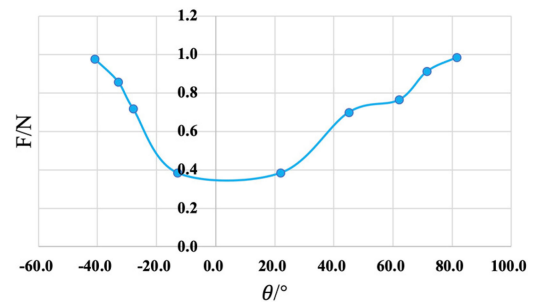


**Fig. 10.** Nonsymmetry of the resistance force of the soft actuator concerning the direction of the deformation.

the virtual finger touched the ball. The human user is able to feel the contact sensation that is collocated with the graphics display. The soft-rigid coupled linkage can not only allow the free movement of the fingers when the soft actuators are not in action, but also transmit the force to the fingertips when the actuator is inflated. The proposed glove is effective to meet the demand of both the free and the constrained space.

#### V. EXPERIMENTS

##### A. Mechanical Behavior of the Soft Actuator

Two experiments were performed to characterize the mechanical behavior of the soft actuator. The first experiment aimed to measure the resistance forces produced by the actuator when it was manually bent under either positive or negative direction. It should be noted that there was no inflated air pressure into the actuator. As shown in **Fig. 9**, one end of the soft actuator was fixed and a force sensor (FSG15N1A, Honeywell Inc., USA) was attached to the tip of the actuator. A user moved the force sensor to deform the actuator. The force sensor was moved at a constant rotating speed while the tip of the force sensor was always perpendicular to the axis of the actuator. The force signal under different bending angles was recorded.

Experimental results in **Fig. 10** illustrate the nonsymmetry of the resistance force of the soft actuator concerning the deformation. To ensure free-space sensation, the resistance force needs to be smaller than the predefined threshold (e.g., 1 N in our design). Then, we determine the prebending angles of the actuator at the two extreme states to be  $80^\circ$  and  $-40^\circ$ , respectively.

In the second experiment, we aimed to measure the effect of the prebending on the resistance force that can be overcome by the actuator. As shown in **Fig. 11**, one end of the actuator was fixed, and initial air pressure was inflated into the actuator to produce a prebending. Then, a force sensor (FSG15N1A,



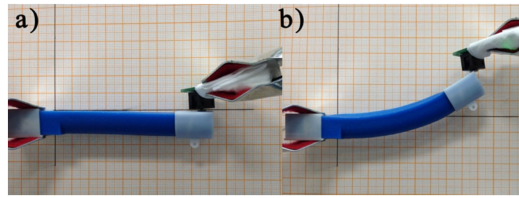


Fig. 11. Different initial air pressure lead to different prebending values of the free end of the actuator. (a) 0 KPa. (b) 83 KPa.

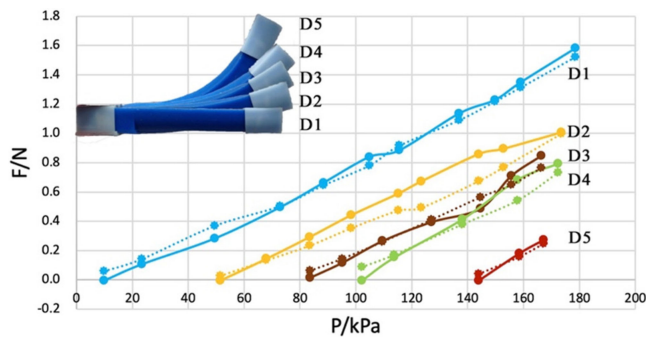


Fig. 12. Relationship between the contact force and the air pressure under five different prebending deformation values. Dashed and solid lines represent FEA and experimental results, respectively.

Honeywell Inc., USA) was mounted to the free end of the actuator, while iron support was used to fix the force sensor. The contact force between the sensor and the end of the actuator was adjusted to be zero. Starting from an initial pressure, the air pressure was increased, and the contact force was measured. Using this experiment, we aimed to measure the ability of the actuator to overcome external forces on its free end.

Five levels of initial air pressure were measured, including 10, 51, 83, 102, and 144 kPa, respectively. As shown in Fig. 11(a) and (b), different initial air pressures led to different prebending of the free end of the actuator.

As shown in Fig. 12, if the actuator has zero prebending, the contact force increases with the increase of the air pressure. However, when the actuator has a prebending, the contact force kept being zero until the inflated pressure became larger than the initial pressure producing the prebending. Only after the inflated pressure is larger than the initial pressure, the output force of the actuator could increase with the increase of air pressure. In the other word, with the increase of the air pressure, the glove cannot provide output force unless the deformation of the actuator caused by the inflated pressure is larger than the prebending deformation. This result reveals the pros and cons of using the prebending approach, i.e., although it is beneficial to improve the back drivability in simulating free space, it leads to the cost of reduced force range in simulating the constrained space.

Furthermore, with the increase of the prebending, in order to achieve the same driving force, larger air pressure is needed. For example, as shown in Fig. 12, in order to output 0.2 N, the required pressures for the five different prebending values are 37, 72, 104, 118, and 160 kPa, respectively.

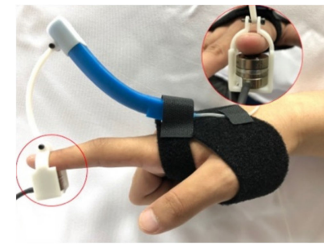


Fig. 13. Setup to measure the force exerted by the rigid rod on the user's fingertip, while the zoomed view shows the force sensor.

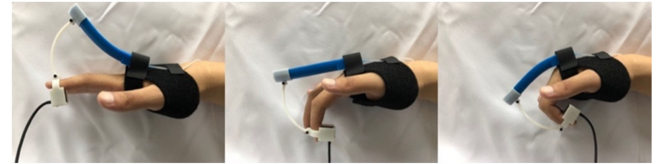


Fig. 14. Measuring fingertip forces during repeated grasping motion.

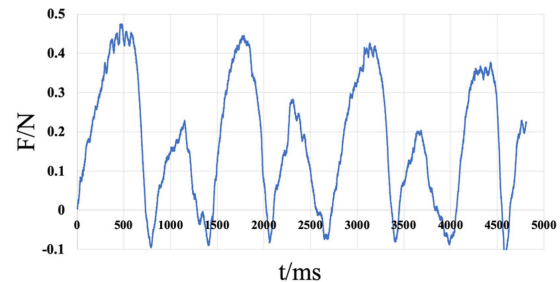


Fig. 15. Measured force signal during the free space test.

The relative error between the FEA and experimental results are shown in Fig. 12, in which the error is less than 15% for all the five prebending deformation conditions.

## B. Performance Evaluation of the Soft Glove

Experiments were performed to measure the performance of the glove in both free space and constrained space. As shown in Fig. 13, a Nano 17 force sensor was utilized to measure the force exerted by the rigid rod on user's fingertip. The force sensor was mounted between a fingertip and the fingertip. Using this setup, user can freely rotate his/her finger and the feedback force on fingertip can be measured with respect to different air pressures and different configurations of the fingers. The resolution of the force sensor is 0.003 N and the sample rate of the force sensor is 1 kHz.

In the free space experiment, the air pressure was zero, and the user performed repeated opening and closing action, as shown in Fig. 14. Using the ATI force sensor, the dynamic data of the contact force in free space were recorded.

As shown in Fig. 15, our experimental results show that the resistance force in free space is about 0.48 N, which is much less than the expected 1 N. The existing resistance is mainly due to the stiffness of the soft actuator and the friction

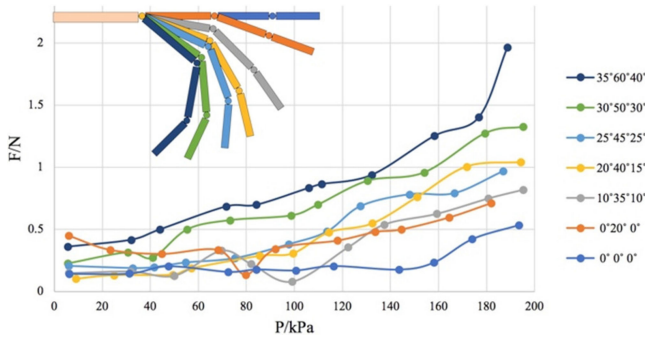


Fig. 16. Force signal under different pressures for each posture.

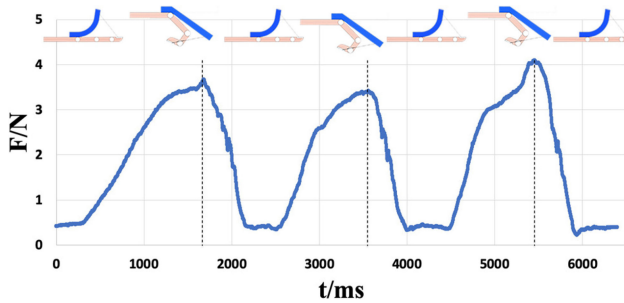


Fig. 17. Measured force signal during the constrained space test.

force of the rotational joints in the transmission mechanism. One potential approach to further reduce this force is to introduce active compensation of the resistance force by air pressure control.

For simulating the constraint space, as shown in Fig. 16, a user was required to rotate his index finger to one of the seven typical finger postures, which are defined by the combinations of the angle of the three finger joints ( $\theta_1$ ,  $\theta_2$ , and  $\theta_3$ ). In each finger posture, the air pressure was controlled to increase the feedback force on the fingertip. For each finger posture, the force signal under 12 levels of air pressures are measured. For all the finger postures, the results show a proportional relationship between the force and the air pressure. Furthermore, for a given air pressure, the force increases along with the increase of the finger joints angle, which imply that the mechanism can produce a larger force at a grasping posture than at the finger extension posture.

Furthermore, the maximum force magnitude of the glove was measured. In order to ensure the safety of the soft actuator (e.g., not to be exploded), a relatively safe pressure was used (i.e., 216.67 kPa) to measure the contact force on the fingertip. During the test, a user put on the glove and performed three cycles of “bend–stretch” movements. The force data recorded by the force sensor are shown in Fig. 17. The maximum feedback force is about 4.09 N. The results show that the device is able to provide a feedback force sufficient for simulating daily grasping tasks.

Further experiments were performed to measure the dynamic response of the glove. The delay of the electro-pneumatic regulator is about 100 ms. As the simulated stiffness was directly

TABLE II  
USER RATING RESULTS

Question	Score (7-point)
Comfortable wearing of gloves	5.2
Fatigue degree after wearing a long time (over 30min)	4.5
The distinct sensation of the force feedback in the free space and the constraint space	4.8
The response of the virtual reality system	5.2
The realism of gloves in virtual reality.	4.8

Perceptual	Big	81	16	4
	Middle	17	64	15
	Small	2	20	81
		Big	Middle	Small
Actual				
(a)				

Perceptual	Big (hard)	65	10	1	
	Small (hard)	3	57	9	1
	Big (soft)	2	2	57	6
	Small (soft)		1	3	63
		Big (hard)	Small(hard)	Big (soft)	Small (soft)
		Actual			
		(b)			

Fig. 18. Results. (a) First experiment. (b) Second experiment.

determined by the sampling and controlling rate of the haptic control system [27], this result implies that the glove is more suitable to simulate soft virtual objects.

In order to evaluate the performance of the glove, we added finger motion tracking to the glove and performed user studies to test how easily and reliably users can discriminate between virtual objects with different sizes and different stiffness. Ten participants were recruited to perform two experiments. In the first experiment, participants need to distinguish three virtual spheres with different sizes (i.e., the radius is 2.5, 5, and 10 cm, respectively), while the stiffness of all three spheres is 100 N/m. Each participant was given three minutes to get familiar with the glove and the three spheres, then the participant performed 30 trials in the formal experiment, which includes ten trials for each of the three target spheres. The three spheres are randomly displayed for each trial.

In the second experiment, participants need to distinguish two different sized spheres (i.e., radius 35 mm, 100 cm) with different stiffness (6 N/m, 120 N/m). For each of the four conditions (2 size levels \* 2 stiffness levels), 7 trials are displayed to the participants in a randomized sequence.

After the two experiments, the participants were required to fill in a questionnaire form for evaluating the performance of the gloves with the 7-point Likert scale (zero refers lowest, seven refers to highest), including five questions, as shown in Table II.

The experimental results are shown as the confusion matrix in Fig. 18. The value in each unit represents the number of the correctly distinguished trials. It can be found that the value of the units along the diagonal line is significantly greater than the value of other units. This illustrates that the proposed glove can support users to correctly distinguish virtual spheres with the defined sizes and stiffness levels. Nevertheless, more efforts are needed to improve the performance of the proposed glove further, and thus, to obtain a higher correct rate of users' perception experiments. The results of the questionnaire are shown in Table II.



## C. Discussions

By using the soft bending actuator and the single-link transmission mechanism, the proposed glove has a lightweight of 31.23 g per finger, which ensure that users will be free of fatigue for performing long term grasping/touching manipulation tasks. In the meantime, the soft connection between the actuator and the user's palm provides comfortable sensations, which avoid the hard contacts of classic rigid parts with users' skin. Last but not the least, the soft actuator will not injure users' finger even in the event of system failure. For example, when the air pressure exceeds the allowable pressure of the actuator, the soft actuator would leak rather than explode due to the use of fiber. This ensures the safety of the user's finger joints.

The proposed glove allows a wide range of finger grasping motion. The soft actuators and the mechanism are all mounted in the dorsal side, so the motion range of the fingers would not be constrained by the glove. In both free and constrained space, the glove can support full hand opening and closing.

The response time of the proposed glove is more than 130 ms, which is mainly due to the delay of the pneumatic control system to produce the deformation of the soft bending actuator. In the future, we will adopt novel pneumatic control systems to speed up the system response [28], along with optimizing the shape of the cavity structure of the soft actuator to improve the system response.

Nevertheless, rigorous work needs to be performed to achieve a high-performance force feedback glove. First of all, one limitation of the proposed prototype is that the dynamic response of the glove needs to be improved. It is necessary to study the quantified impact of the diameter and the length of the air tubes on the responsiveness of the glove. Second, by adjusting the mounting position of the base part of the soft actuator on the palm, the proposed glove can adapt to a certain range of human hands with different sizes. In the future, we can further enlarge the adaptive range of the glove to different hand sizes by introducing new mechanical structures with an adjustable length of the soft actuator and/or the rigid rod.

## VI. CONCLUSION

In this article, we presented empirical models for designing force feedback gloves using pneumatically powered fiber-reinforced soft bending actuators. A soft-rigid linkage mechanism was synthesized to meet the contradictive requirements for both free space and constrained space simulations. Specifically, a positive prebending deformation of the soft actuator was experimentally determined to ensure a small back drive force for simulating free-space sensation. In the other aspect, to ensure a large workspace of the glove and produce a larger feedback force on the fingertip, the shape and parameters of the rigid rod were synthesized to ensure full open/closure of the finger without any mechanical interference between the rod and the users' finger. Furthermore, the glove can provide distinct force feedback between free and constrained space. For free space, the maximum back drive force is 0.48 N, while the fingertip force reaches up to 4.09 N for simulating the constrained space. Experiments also indicate that the glove is easy to put ON/OFF.

In the future, we plan to extend the proposed modular solution to all five fingers with finger motion tracking and add distributed tactile sensing on the palm and carry out a user study to evaluate the performance of the soft glove for simulating diverse grasping tasks.

## REFERENCES

- [1] T. Endo *et al.*, "Five-fingered haptic interface robot: HIRO III," *IEEE Trans. Haptics*, vol. 4, no. 1, pp. 14–27, Jan./Feb. 2011.
- [2] L. Liu, S. Miyake, K. Akahane, and M. Sato, "Development of string-based multi-finger haptic interface SPIDAR-MF," in *Proc. Int. Conf. Artif. Reality Telexistence*, 2014, pp. 67–71.
- [3] S. Walairacht, M. Ishii, Y. Koike, and M. Sato, "Two-handed multi-fingers string-based haptic interface device," *IEICE Trans. Inf. Syst. D*, vol. 84, no. 3, pp. 365–373, Mar. 2001.
- [4] CyberGlove Systems, Cybergrasp. 2013. [Online]. Available: <http://www.cyberglovesystems.com/>
- [5] T. Koyama, I. Yamano, K. Takemura, and T. Maeno, "Multifingered exoskeleton haptic device using passive force feedback for dexterous teleoperation," in *Proc. IEEE/RSJ Int. Conf. Intell. Robots Syst.*, 2002, pp. 2905–2910, vol. 3.
- [6] L. Jiang, "Portable haptic feedback for training and rehabilitation," Ph.D. dissertations, Dept. Mech. Eng., Gradworks, Londonderry, U.K., 2009.
- [7] S. H. Winter and M. Bouzit, "Use of magnetorheological fluid in a force feedback glove," *IEEE Trans. Neural Syst. Rehabil. Eng.*, vol. 15, no. 1, pp. 2–8, Apr. 2007.
- [8] J. Blake and H. B. Gurocak, "Haptic glove with MR brakes for virtual reality," *IEEE/ASME Trans. Mechatronics*, vol. 14, no. 5, pp. 606–615, Oct. 2009.
- [9] M. Bouzit, G. Burdea, G. Popescu, and R. Boian, "The rutgers master II-new design force-feedback glove," *IEEE/ASME Trans. Mechatronics*, vol. 7, no. 2, pp. 256–263, Jun. 2002.
- [10] I. Zubrycki and G. Granosik, "Novel haptic glove-based interface using jamming principle," in *Proc. 10th Int. Workshop Robot Motion Control*, Jul. 2015, pp. 46–51.
- [11] T. M. Simon, R. T. Smith, and B. H. Thomas, "Wearable jamming mitten for virtual environment haptics," in *Proc. ACM Int. Symp. Wearable Comput.*, 2014, pp. 67–70.
- [12] H. In, B. B. Kang, M. K. Sin, and K. J. Cho, "Exo-Glove: A wearable robot for the hand with a soft tendon routing system," *IEEE Robot. Autom. Mag.*, vol. 22, no. 1, pp. 97–105, Mar. 2015.
- [13] I. Choi, E. W. Hawkes, D. L. Christensen, C. J. Ploch, and S. Follmer, "Wolverine: A wearable haptic interface for grasping in virtual reality," in *Proc. IEEE/RSJ Int. Conf. Intell. Robots Syst.*, 2016, pp. 986–993.
- [14] C. Pacchierotti, S. Sinclair, M. Solazzi, A. Frisoli, V. Hayward, and D. Prattichizzo, "Wearable haptic systems for the fingertip and the hand: Taxonomy, review, and perspectives," *IEEE Trans. Haptics*, vol. 10, no. 4, pp. 580–600, Oct./Dec. 2017.
- [15] D. Wang, M. Song, A. Naqash, Y. Zheng, W. Xu, and Y. Zhang, "Toward whole-hand kinesthetic feedback: A survey of force feedback gloves," *IEEE Trans. Haptics*, vol. 12, no. 2, pp. 189–204, Apr./Jun. 2018.
- [16] H. In, B. B. Kang, M. Sin, and K.-J. Cho, "Exo-glove: Soft wearable robot for the hand with soft tendon routing system," *IEEE Robot. Autom. Mag.*, vol. 22, no. 1, pp. 97–105, Jan./Mar. 2014.
- [17] M. Koo, K. Jung, J. C. Koo, J.-D. Nam, Y. K. Lee, and H. R. Choi, "Development of soft-actuator-based wearable tactile display," *IEEE Trans. Robot.*, vol. 24, no. 3, pp. 549–558, Jun. 2008.
- [18] P. Polygerinos, Z. Wang, K. C. Galloway, R. J. Wood, and C. J. Walsh, "Soft robotic glove for combined assistance and at-home rehabilitation," *Robot. Autom. Syst.*, vol. 73, no. C, pp. 135–143, 2015.
- [19] G. Frediani, D. Mazzei, D. E. De Rossi, and F. Carpi, "Wearable wireless tactile display for virtual interactions with soft bodies," *Frontiers Bioengineering Biotechnology*, vol. 2, pp. 1–7, 2014.
- [20] S. Jadhav *et al.*, "Soft robotic glove for kinesthetic haptic feedback in virtual reality environments," *Electron. Imag.*, no. 3, pp. 19–24, 2017.
- [21] S. Yun *et al.*, "Exo-Glove PM: An easily customizable modularized pneumatic assistive glove," *IEEE Robot. Autom. Lett.*, vol. 2, no. 3, pp. 1725–1732, Jul. 2017.
- [22] P. Polygerinos *et al.*, "Towards a soft pneumatic glove for hand rehabilitation," in *Proc. IEEE/RSJ Int. Conf. Intell. Robot. Syst.*, Tokyo, Japan, Nov. 2013, pp. 1512–1517.

- [23] P. Polygerinos, K. C. Galloway, E. Savage, M. Herman, K. O' Donnell, and C. J. Walsh, "Soft robotic glove for hand rehabilitation and task specific training," in *Proc. IEEE Int. Conf. Robot. Autom.*, 2015, pp. 2913–2919.
- [24] Y. Zhang, D. Wang, Z. Wang, Y. Wang, L. Wen, and Y. Zhang, "A two-fingered force feedback glove using soft actuators," in *Proc. IEEE Haptics Symp.*, San Francisco, CA, USA, Mar. 25–28, 2018, pp. 186–191.
- [25] K. Salisbury, D. Brock, T. Massie, N. Swarup, and C. Zilles, "Haptic rendering: programming touch interaction with virtual objects," in *Proc. Symp. Interactive 3-D Graph.*, 1995, pp. 123–130.
- [26] P. Polygerinos *et al.*, "Modeling of soft fiber-reinforced bending actuators," *IEEE Trans. Robot.*, vol. 31, no. 3, pp. 778–789, Jun. 2015.
- [27] J. E. Colgate and J. M. Brown, "Factors affecting the Z-width of a haptic display," in *Proc. IEEE Int. Conf. Robot. Autom.*, 1994, vol. 4, pp. 3205–3210.
- [28] R. Yan *et al.*, "OriSnake: Design, fabrication and experimental analysis of a 3-D origami snake robot," *IEEE Robot. Autom. Lett.*, vol. 3, no. 3, pp. 1993–1999, Jul. 2018.



**Ziqi Wang** was born in Xinzhou, China. He received the B.S. degree in mechanical engineering from the School of Mechanical Engineering and Automation, Beihang University, Beijing, China, in 2018, where he is currently working toward the master's degree.

His research interests include virtual reality and haptic device.



**Dangxiao Wang** (M'05–SM'13) received the Ph.D. degree in mechanical engineering from Beihang University, Beijing, China, in 2004.

He is currently a Professor in Mechanical Engineering and the Deputy Director of the State Key Laboratory of Virtual Reality Technology and Systems in Beihang University. His research interests include haptic rendering, NeuroHaptics, and medical robotic systems.

Prof. Wang was the Chair of Executive Committee of the IEEE Technical Committee on Haptics (IEEE TCH) from 2014 to 2017.



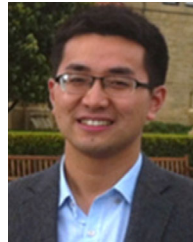
**Yu Zhang** was born in Hunchun China. He received the B.S. degree in mechanical engineering from the School of Energy and Power Engineering, Beihang University, Beijing China, in 2018.

His research interests include robotics, human machine interaction, and haptic device.



**Jiaqi Liu** received the B.S. degree in mechanical engineering from the School of Mechanical Engineering and Automation, Beihang University, Beijing, China, in 2018, where he is currently working toward the master's degree.

His research interests include soft gripper, soft robotic arm, and stretchable sensor.



**Li Wen** received the Ph.D. degree in mechanical engineering from Beihang University, Beijing, China, in 2011.

He is an Associate Professor in Mechanical Engineering with the Beihang University. His research interests include bio-inspired robotics, soft robotics, and comparative biomechanics.

Dr. Wen received the National Science Foundation Excellent Scholar Award and leads the Chinese National Science Foundation Key Project on underwater soft robotics. He is an

Associate Editor of the IEEE Robotics and Automation Letters.



**Weiliang Xu** (SM'99) received the B.E. degree in manufacturing engineering and the M.E. degree in mechanical engineering from Southeast University, Nanjing, China, in 1982 and 1985, respectively, and the Ph.D. degree in mechatronics and robotics from the Beijing University of Aeronautics and Astronautics, Beijing, China, in 1988.

He joined The University of Auckland, Auckland, New Zealand, in 2011, as Chair in Mechatronics Engineering.



**Yuru Zhang** (M'95–SM'08) received the Ph.D. degree in mechanical engineering from Beihang University, Beijing, China, in 1987.

Her research interests include haptic human-machine interface, medical robotic systems, robotic dexterous manipulation, and virtual prototyping.

Prof. Zhang is an Associate Editor of the IEEE Robotics and Automation Letters.